Probing the nature of the anticharmed-strange pentaquark states

Reporter: Xue-Jie Liu (刘雪杰)

Henan normal university(河南师范大学)

Collaborators: Jia-Lun Ping (平加伦) Hong-Xia Huang(黄虹霞)
Dian-yong Chen (陈殿勇)

Based on: Phys. Rev. D **110** (2024) 074001
ArXiv: 2407.05598

第十届手征有效场论研讨会@南京

2025-10-19

Outline

- Backgroud and motivation
- Quark Model and Calculation Method
- Results of the Anticharmed-Strange Pentaquark Candidates
- Summary

Background and motivation

➢ Conventional hadron

✓ Mesons($\bar{q}q$)

✓ Baryons(qqq)

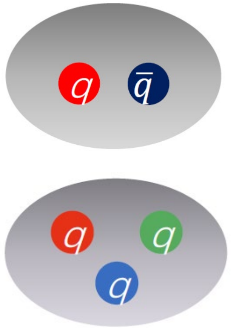

➢ Exotic hadron states

✓ Multiquarks(qqqq….)

✓ Hybrids(qqg)

✓ Glueballs(gg,ggg….)

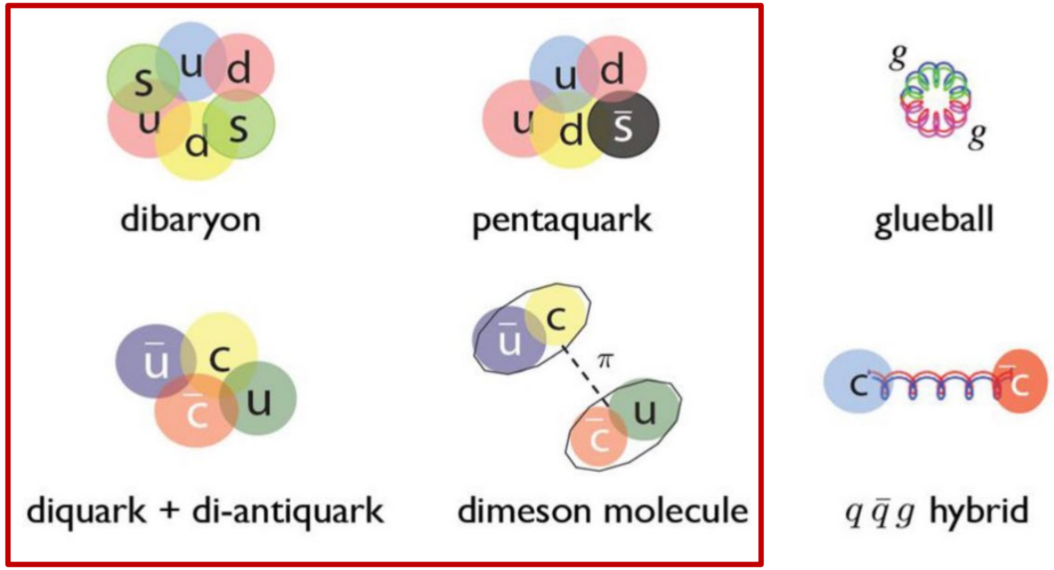

Searching for exotic hadron states remains an important ongoing research area in hadron physics!

Background and motivation

➢ Experimental breakthroughs

- X(3872) was first observed by Belle Collabortaion [Belle] PRL91,262001 (2003)

----the study of multiquark states has entered upon a new era

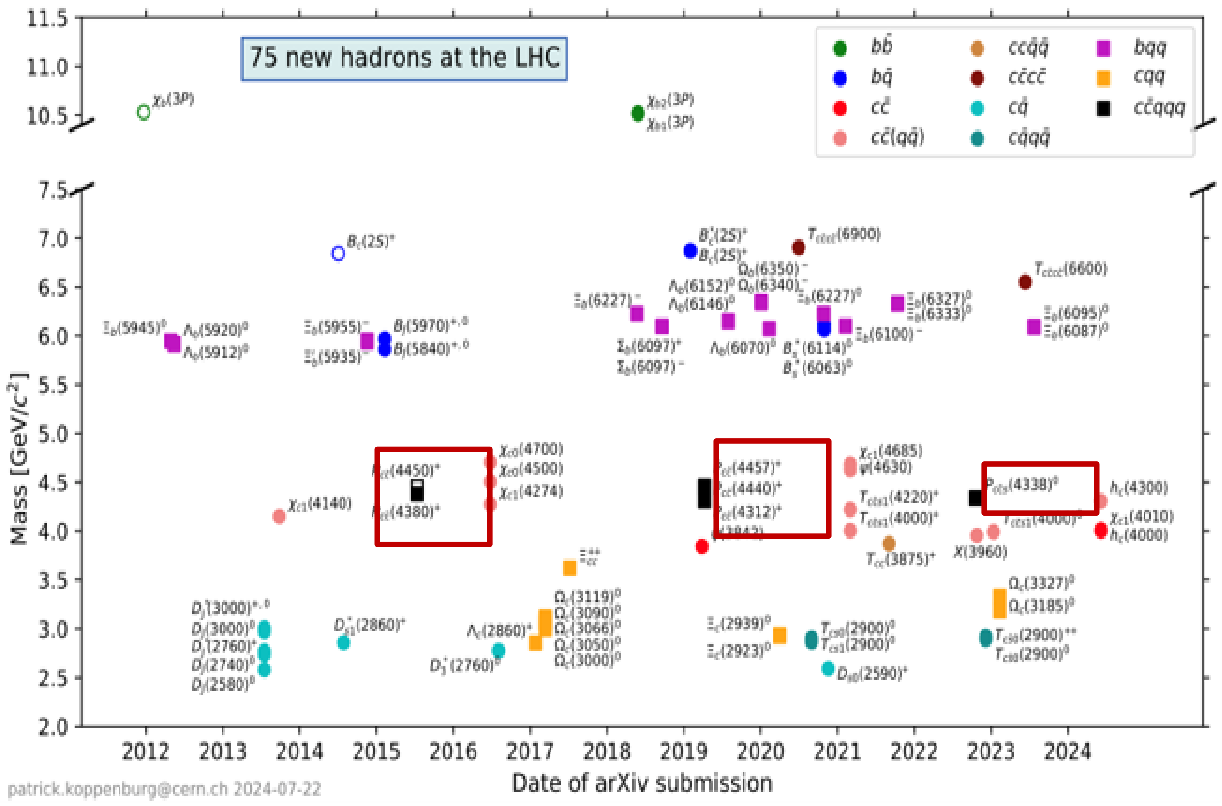

- Since 2015, a series of hidden-charm pentaquark states (P_c, P_{cs}) have been observed by the LHCb Collabortaion
- Theoretical interpretations:
  - ✓ molecular states:
    H. X. Huang et al, Phys.Rev.D 99 (2019) 1, 014010.
    H. X. Chen et al, Phys.Rev.D 100 (2019) 5, 051501.
    M. Z. Liu, et al, Phys. Rev. Lett. 122, 242001 (2019).
    …
  - ✓ Compact states:
    Ahmed Ali et al. Phys.Lett.B 793 (2019) 365-371.
    Z.-G. Wang, Int. J. Mod. Phys. A 35, 2050003 (2020).
    A. Ali, I. Ahmed et al. J. High Energy Phys. 10 (2019) 256.
    …
  - ✓ No-resonant: threshold effect(cusp, triangle singularity)
    F.-K. Guo et al, Phys. Rev. D 92, 071502 (2015).
    S. X. Nakamura, Phys. Rev. D 103, L111503 (2021).
    …

Background and motivation

- **LHCb Collaboration utilized proton-proton collision data for the first time to study the $\Lambda_b^0 \to \Lambda D^+ D^-$ at nearly 13 TeV energy levels.**

[LHCb] *JHEP* 07 (2024) 140

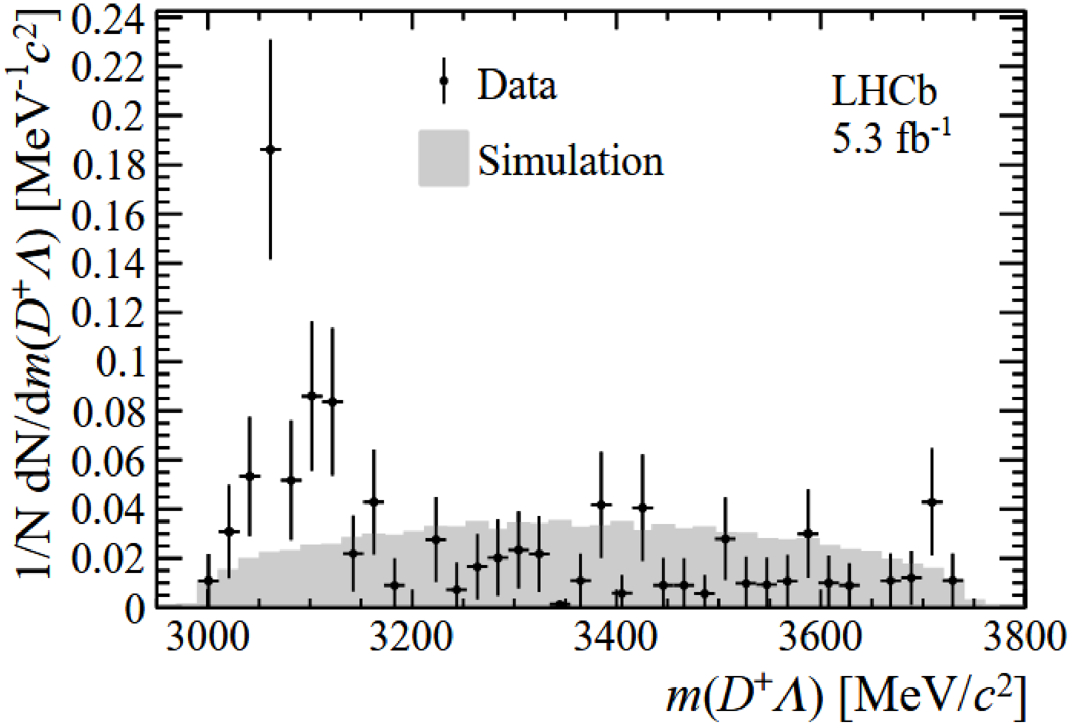

- Form the invariant mass distributions of ΛD^+,a rich presence of intermediate resonances in the decay.

- These hints imply the possible existence of open-charm pentaquark states with quark content $\bar{c}sqqq$.

Our goal: To predict the stable states and decay properties of the $\bar{c}sqqq$

Quark model and calculation method

➢ Quark delocalization color screening model (QDCSM)

- QDCSM was developed by Nanjing-Los Alamos collaboration in 1990s aimed to multi-quark study. (PRL 69, 2901, 1992)
- Two new ingredients

  quark delocalization (orbital excitation)
  color screening (color structure)

- Apply to the study of baryon-baryon interaction and dibaryons

  deuteron, d*, NN, N Λ, NΩ,…

- Apply to the study of baryon-meson interaction and pentaquarks

  NK, Nπ, P_c,…

Quark model and calculation method

$$
\begin{aligned}
H &= \sum_{i=1}^{5}\left(m_i + \frac{p_i^2}{2m_i}\right) - T_c + \sum_{i<j}[V^G(r_{ij}) + V^\chi(r_{ij}) + V^C(r_{ij})],\\
V^G(r_{ij}) &= \frac{1}{4}\alpha_s\lambda_i\cdot\lambda_j\left[\frac{1}{r_{ij}} - \frac{\pi}{2}\left(\frac{1}{m_i^2} + \frac{1}{m_j^2} + \frac{4\sigma_i\cdot\sigma_j}{3m_im_j}\right)\delta(r_{ij}) - \frac{3}{4m_im_jr_{ij}^3}S_{ij}\right],\\
V^\chi(r_{ij}) &= \frac{1}{3}\alpha_{ch}\frac{\Lambda^2}{\Lambda^2 - m_\chi^2}m_\chi\left\{\left[Y(m_\chi r_{ij}) - \frac{\Lambda^3}{m_\chi^3}Y(\Lambda r_{ij})\right]\sigma_i\cdot\sigma_j + \left[H(m_\chi r_{ij}) - \frac{\Lambda^3}{m_\chi^3}H(\Lambda r_{ij})\right]S_{ij}\right\}\mathbf{F}_i\cdot\mathbf{F}_j, \qquad \chi = \pi, K, \eta,\\
V^C(r_{ij}) &= -a_c\lambda_i\cdot\lambda_j[f(r_{ij}) + V_0],\\
f(r_{ij}) &= \begin{cases} r_{ij}^2 & \text{if } \ i, j \text{occur in the same baryon orbit},\\ \frac{1-e^{-\mu_{ij}r_{ij}^2}}{\mu_{ij}} & \text{if } \ i, j \text{occur in different baryon orbits},\end{cases}\\
S_{ij} &= \frac{(\sigma_i\cdot\mathbf{r}_{ij})(\sigma_j\cdot\mathbf{r}_{ij})}{r_{ij}^2} - \frac{1}{3}\sigma_i\cdot\sigma_j, \qquad\qquad (1)
\end{aligned}
$$

Quark model and calculation method

➢ Resonating group method (RGM)

J. A. Wheeler, Phys. Rev. **52**, 1107-1122 (1937)

- In RGM, the multiquark wave function is approximated by the cluster wave function

$$\Psi = \mathcal{A}\left[[\phi_{B_1}(\vec{\rho}_1, \vec{\lambda}_1)\phi_{B_2}(\vec{\rho}_2, \vec{\lambda}_2)]^{[\sigma]IS}\chi(R)Z(\vec{R}_C) \right],$$

- Variational principle

$$\langle \delta\Psi'' | H - E | \Psi' \rangle = 0.$$

$$\Psi'' = \int \mathcal{A}\left[\phi_1(\rho_1, \lambda_1)\phi_2(\rho_2, \lambda_2)\delta(R - R'')\right]\chi(R'')dR'',$$

$$\Psi' = \int \mathcal{A}\left[\phi_1(\rho_1, \lambda_1)\phi_2(\rho_2, \lambda_2)\delta(R - R')\right]\chi(R')dR',$$

$$\delta\Psi'' = \int \mathcal{A}\left[\phi_1(\rho_1, \lambda_1)\phi_2(\rho_2, \lambda_2)\delta(R - R'')\right]\delta\chi(R'')dR''.$$

- The relative motion wave function satisfies the following RGM equation

$$\int H(R'', R')\chi(R')dR' = E\int N(R'', R')\chi(R')dR',$$

$$H(R'', R') = \langle [\phi_1\phi_2\delta(R - R'')] | H | \mathcal{A}[\phi_1\phi_2\delta(R - R')] \rangle,$$
$$N(R'', R') = \langle [\phi_1\phi_2\delta(R - R'')] | \mathcal{A}[\phi_1\phi_2\delta(R - R')] \rangle.$$

$\Longrightarrow$

$$H(R'', R') = H^D(R'', R')\delta(R - R'') + H^{EX}(R'', R'),$$
$$N(R'', R') = N^D(R'', R')\delta(R - R'') + N^{EX}(R'', R').$$

Quark model and calculation method

➢ Kohn-Hulthen-Kato (KHK) variational method

M. Kamimura, Prog. Theor. Phys. Suppl. 62(1977) 236

$$u_t(R) = \sum_{i=0}^{n} c_i u_i(R)$$

$$u_i(R) = \begin{cases} \alpha_i u_i^{(in)}(R), & R < R_c, \\ (h_L^{(-)}(k,R) + s_i h_L^{(+)}(k,R))R, & R > R_c \end{cases}$$

$$\frac{u_i^{(in)}(R)}{R} = \sqrt{4\pi}(\frac{3}{2\pi b^2})^{\frac{3}{4}} e^{-\frac{3}{4b^2}(R^2+r_i^2)} i^L j_L(-i\frac{3}{2b^2}Rr_i)$$

$$\sum_{i=0}^{n} c_i = 1, \qquad \sum_{i=0}^{n} c_i s_i = S_t.$$

$$\Downarrow$$

$$c_0 = 1 - \sum_{i=1}^{n} c_i \quad \Longrightarrow \quad u_t(R) = u_0(R) + \sum_{i=1}^{n} c_i(u_i(R) - u_0(R))$$

Quark model and calculation method

$$\langle \delta\Psi' | H - E | \Psi \rangle = 0$$

$$\sum_{j=1}^{n} \mathcal{L}_{ij} c_j = \mathcal{M}_i, (i = 1 \sim n)$$

$$\boxed{\begin{gathered} \mathcal{L}_{ij} = \mathcal{K}_{ij} - \mathcal{K}_{i0} - \mathcal{K}_{0j} + \mathcal{K}_{00}, \\ \mathcal{M}_i = \mathcal{K}_{00} - \mathcal{K}_{i0} \\ \mathcal{K}_{ij} = \langle \phi_A(\xi_A)\phi_B(\xi_B)u_i(R)/R \cdot Y_{LM}(\hat{R}) | H - E | \mathcal{A}[\phi_A(\xi_A)\phi_B(\xi_B)u_j(R)/R \cdot Y_{LM}(\hat{R})] \rangle \end{gathered}}$$

$$\sum_{i=0}^{n} c_i s_i = S_t \qquad S_L = |S_L| e^{2i\delta_L}$$

$$c_i \Longrightarrow S_t \Longrightarrow S_L \Longrightarrow \delta_L$$

$$\sigma_L = \frac{4\pi}{k^2} \cdot (2l+1) \cdot \sin^2 \delta_L$$

Results of the Anticharmed-Strange Pentaquark

- Here, we only consider the S-wave channels for the anticharmed-strange pentaquarks

TABLE I. The relevant channels for all possible states with different J^P quantum numbers.

	$S=\frac{1}{2}$		$S=\frac{3}{2}$		$S=\frac{5}{2}$	
$I=\frac{1}{2}$	$\Lambda\bar{D}$	$\Lambda\bar{D}^*$	$\Lambda\bar{D}^*$	$\Sigma\bar{D}^*$	$\Sigma^*\bar{D}^*$	
	$\Sigma\bar{D}$	$\Sigma\bar{D}^*$	$\Sigma^*\bar{D}$	$\Sigma^*\bar{D}^*$		
	$\Sigma^*\bar{D}^*$	ND_s^-	ND_s^{*-}			
	ND_s^{*-}					
$I=\frac{3}{2}$	$\Sigma\bar{D}$	$\Sigma\bar{D}^*$	$\Sigma\bar{D}^*$	$\Sigma^*\bar{D}$	$\Sigma^*\bar{D}^*$	ΔD_s^{*-}
	$\Sigma^*\bar{D}^*$	ΔD_s^{*-}	$\Sigma^*\bar{D}^*$	ΔD_s^-		
			ΔD_s^{*-}			

Results of the Anticharmed-Strange Pentaquark

➢ The effective potential analysis

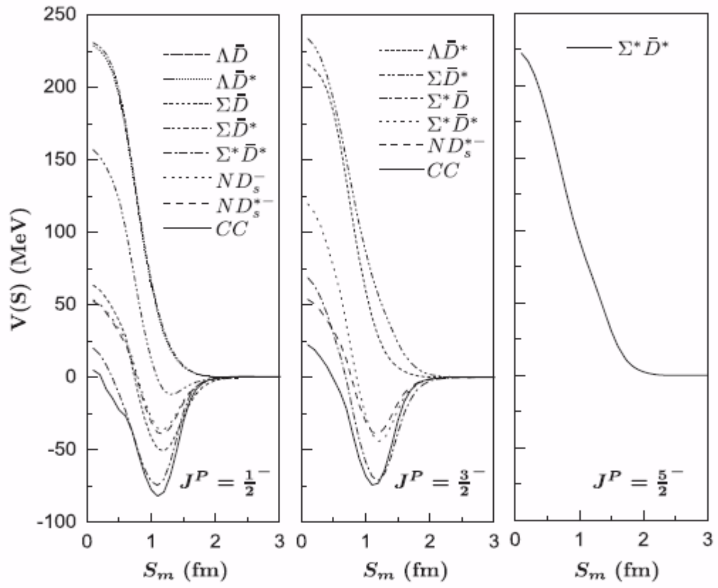

FIG. 1. The effective potentials defined in Eq. (12) for different channels of the anticharmed-strange pentaquark systems with $I = 1/2$ in QDCSM. *CC* stands for the effective potentials after considering the all-channel coupling.

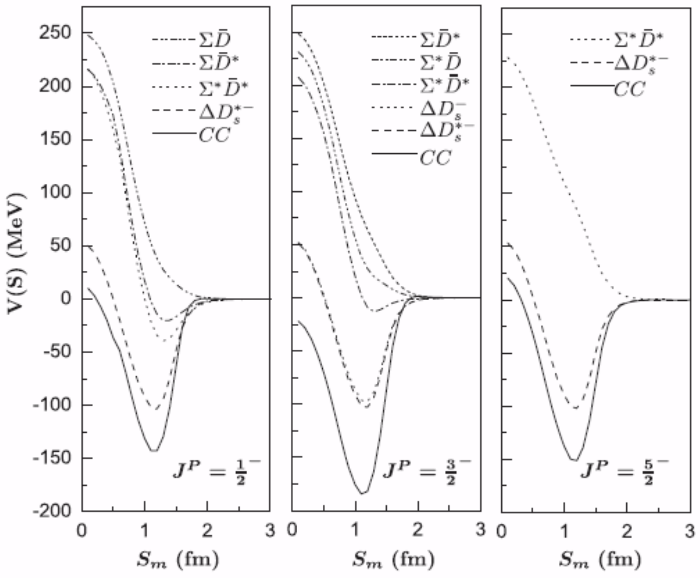

FIG. 2. The effective potentials defined in Eq. (12) for different channels of the anticharmed-strange pentaquark systems with $I = 3/2$ in QDCSM. *CC* stands for the effective potentials after considering the all-channel coupling.

- Strongest attraction:
  For $J^P = 1/2^-$, the $\Sigma^*\bar{D}^*$ and $\Sigma\bar{D}$ channels are the most attractive.
  For $J^P = 3/2^-$, the $\Sigma^*\bar{D}$ channel shows significant attraction.
- Replusive channels:
  channels like $\Lambda\bar{D}$ and $\Lambda\bar{D}^*$ are repulsive.

- Strongest attraction:
  channels involving the Δ baryon, such as ΔD_s^* and ΔD_s^-, consistently show the strongest attraction.
- Replusive channels:
  channels like $\Sigma^*\bar{D}^*$ and $\Sigma\bar{D}$ are repulsive.

Crucial role of channel coupling: The resulting attraction after coupling is the strongest, strongly suggesting the presence of bound states

Results of the Anticharmed-Strange Pentaquark

➢ Bound state predictions

TABLE II. The binding energies and the masses of every single channel and those of channel coupling for the pentaquarks with $I = 1/2$. The values are provided in units of MeV.

$I(J^P)$	Channel	E_{sc}	E_{th}^{Model}	E_B	E_{th}^{Exp}	E'_{sc}	E_{cc}/E_B	E'_{cc}
$\frac{1}{2}(\frac{1}{2}^-)$	$\Lambda\bar{D}$	2992	2988	4	3122	3126	2873/-21	2886
	$\Lambda\bar{D}^*$	3027	3023	4	3227	3231		
	$\Sigma\bar{D}$	3101	3102	−1	3058	3057		
	$\Sigma\bar{D}^*$	3140	3137	3	3196	3199		
	$\Sigma^*\bar{D}^*$	3251	3259	−8	3392	3384		
	ND_s^-	2896	2894	2	2907	2909		
	ND_s^{*-}	2910	2908	2	3051	3053		
$\frac{1}{2}(\frac{3}{2}^-)$	$\Lambda\bar{D}^*$	3027	3023	4	3122	3126	2896/-12	3039
	$\Sigma\bar{D}^*$	3141	3137	4	3196	3200		
	$\Sigma^*\bar{D}$	3218	3224	−6	3254	3248		
	$\Sigma^*\bar{D}^*$	3261	3259	2	3392	3394		
	ND_s^{*-}	2910	2908	2	3051	3053		
$\frac{1}{2}(\frac{5}{2}^-)$	$\Sigma^*\bar{D}^*$	3263	3259	4	3392	3396	3263/4	3396

Rms: 1.2 fm
ND_s^-: 96%

Rms: 1.5 fm
ND_s^{*-} : 97%

Results of the Anticharmed-Strange Pentaquark

➢ Bound state predictions

TABLE III. The binding energies and the masses of every single channel and those of channel coupling for the pentaquarks with $I = 3/2$. The values are provided in units of MeV.

$I(J^P)$	Channel	E_{sc}	E_{th}^{Model}	E_B	E_{th}^{Exp}	E'_{sc}	E_{cc}/E_B	E'_{cc}
$\frac{3}{2}(\frac{1}{2}^-)$	$\Sigma\bar{D}$	3106	3102	4	3058	3062	3103/1	3059
	$\Sigma\bar{D}^*$	3140	3137	3	3196	3199		
	$\Sigma^*\bar{D}^*$	3261	3259	2	3392	3394		
	ΔD_s^{*-}	3167	3201	−34	3344	3310		
$\frac{3}{2}(\frac{3}{2}^-)$	$\Sigma\bar{D}^*$	3141	3137	4	3196	3200	3094/-43	3153
	$\Sigma^*\bar{D}$	3228	3224	4	3254	3248		
	$\Sigma^*\bar{D}^*$	3263	3259	4	3392	3394		
	ΔD_s^-	3162	3187	−25	3200	3175		
	ΔD_s^{*-}	3155	3201	−45	3344	3299		
$\frac{3}{2}(\frac{5}{2}^-)$	$\Sigma^*\bar{D}^*$	3263	3259	4	3392	3396	3202/1	3345
	ΔD_s^{*-}	3206	3201	5	3344	3349		

Rms: 2.1 fm
$\Sigma\bar{D}^*$: 97%

Channel coupling is crucial for the formation of bound states

Results of the Anticharmed-Strange Pentaquark

➢ Bound state confirmation

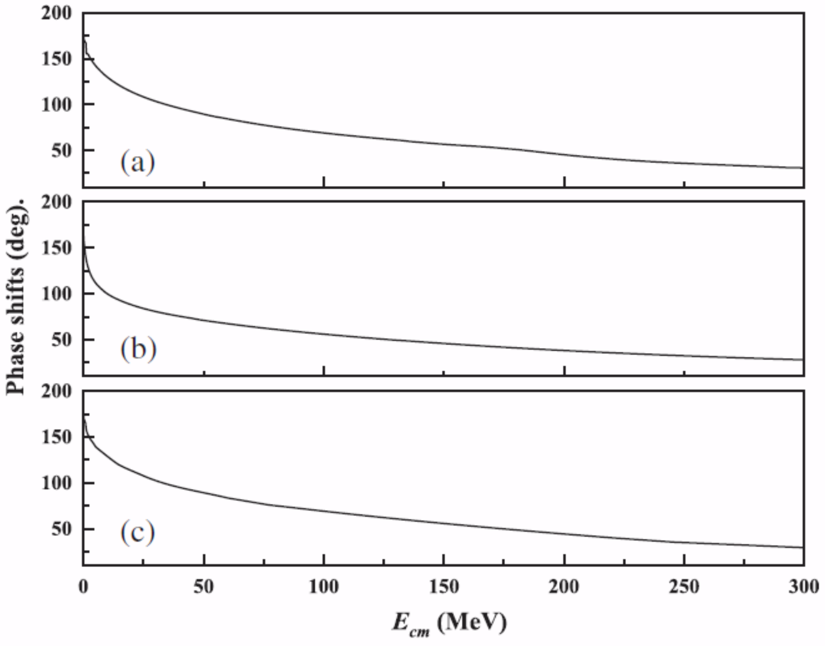

FIG. 3. The phase shifts of the ND_s^- with $I(J^P)=\frac{1}{2}(\frac{1}{2}^-)$, ND_s^{*-} with $I(J^P)=\frac{1}{2}(\frac{3}{2}^-)$, and $\Sigma\bar{D}^*$ with $I(J^P)=\frac{3}{2}(\frac{3}{2}^-)$ in the coupled-channel estimations. (a) Stands for ND_s^- with $I(J^P)=\frac{1}{2}(\frac{1}{2}^-)$, (b) represents ND_s^{*-} with $I(J^P)=\frac{1}{2}(\frac{3}{2}^-)$, (c) stands for $\Sigma\bar{D}^*$ with $I(J^P)=\frac{3}{2}(\frac{3}{2}^-)$.

TABLE IV. The the scattering length a_0, the effective range r_0 and the binding energy E'_B determined by the variation method.

$I(J^P)$	Channel	a_0 (fm)	r_0 (fm)	E'_B (MeV)
$\frac{1}{2}(\frac{1}{2}^-)$	ND_s^-	2.06	0.98	−23.8
$\frac{1}{2}(\frac{3}{2}^-)$	ND_s^{*-}	2.00	1.00	−11.7
$\frac{3}{2}(\frac{3}{2}^-)$	$\Sigma\bar{D}^*$	2.56	1.45	−40.7

- All scattering lengths (a_0) are positive, robustly confirming the presence of bound states
- The binding energies (E'_B) are in agreement with the binding energies obtained from the dynamical calculation

Both the qualitative behavior of the phase shifts and the quantitative analysis of the scattering parameters provide **strong and self-consistent confirmation** for the existence of the three predicted bound states.

Results of the Anticharmed-Strange Pentaquark

➢ Resonance state and decay width

$I(J^P) = \frac{1}{2}\left(\frac{1^-}{2}\right)$

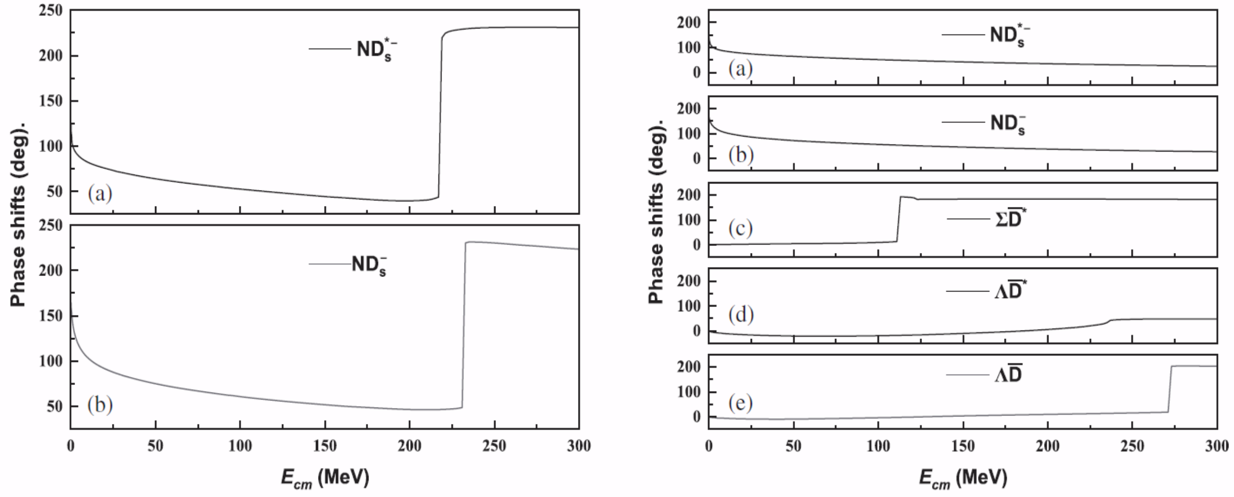

FIG. 4. The phase shifts of the open channels with two-channel coupling for $I(J^P) = 1/2(1/2^-)$ in QDCSM. On the left, (a) corresponds to two channels coupling with $\Sigma\bar{D}$ and ND_s^{*-}, (b) denotes two-channel coupling with $\Sigma\bar{D}$ and ND_s^-. On the right, (a) stands for two-channel coupling with $\Sigma^*\bar{D}^*$ and ND_s^{*-}, (b) indicates two-channel coupling with $\Sigma^*\bar{D}^*$ and ND_s^-, (c) represents two-channel coupling with $\Sigma^*\bar{D}^*$ and $\Sigma\bar{D}^*$, (d) stands for two-channel coupling with $\Sigma^*\bar{D}^*$ and $\Lambda\bar{D}^*$, (e) denotes two-channel coupling with $\Sigma^*\bar{D}^*$ and $\Lambda\bar{D}$.

- $\Sigma\bar{D}$ resonance state was found in the phase shifts of open channel ND_s^- and ND_s^{*-}
- $\Sigma^*\bar{D}^*$ resonance state was seen in the phase shifts of open channel $\Sigma\bar{D}^*$and $\Lambda\bar{D}$

$I(J^P) = \frac{1}{2}\left(\frac{3^-}{2}\right)$

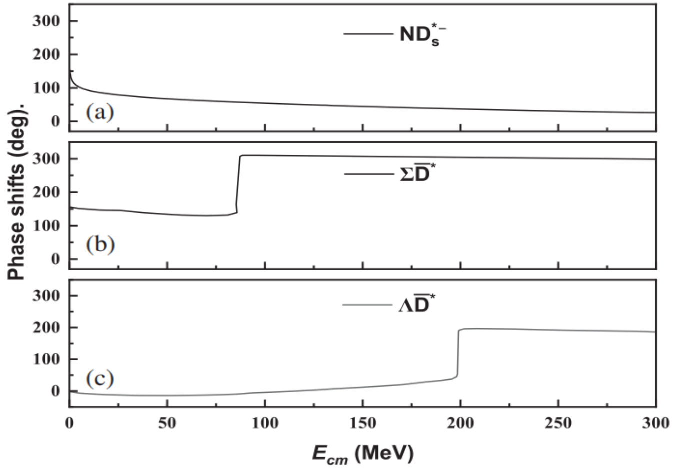

FIG. 6. The phase shifts of the open channels with two channels coupling with a closed channel ($\Sigma^*\bar{D}$) and one open channel (ND_s^{*-}, $\Sigma\bar{D}^*$, $\Lambda\bar{D}^*$) for $I(J^P) = 1/2(3/2^-)$ in QDCSM. (a) represents two-channel coupling with $\Sigma^*\bar{D}$ and ND_s^{*-}, (b) shows two-channel coupling with $\Sigma^*\bar{D}$ and $\Sigma\bar{D}^*$. (c) denotes two-channel coupling with $\Sigma^*\bar{D}$ and $\Lambda\bar{D}^*$.

- $\Sigma^*\bar{D}$ resonance state was obtained in the phase shifts of open channel $\Sigma\bar{D}^*$and $\Lambda\bar{D}^*$

Results of the Anticharmed-Strange Pentaquark

➢ Resonance state and decay width

$$I(J^P) = \frac{1}{2}\left(\frac{1^-}{2}\right)$$

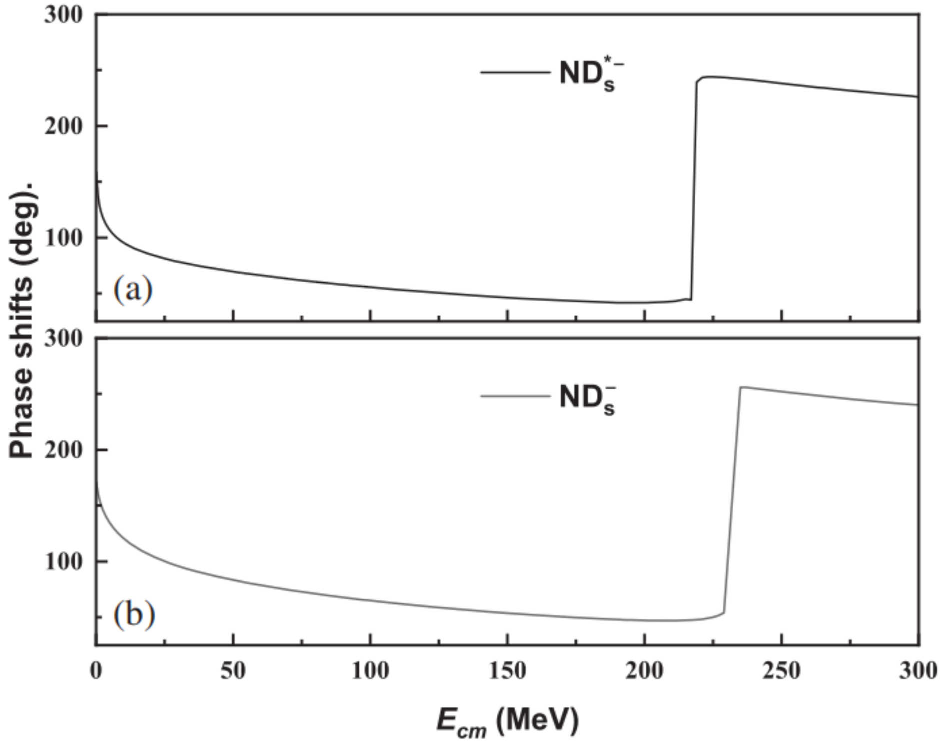

FIG. 5. The phase shifts of the open channels with three channels coupling with two closed channels ($\Sigma\bar{D}$ and $\Sigma^*\bar{D}^*$) and one open channel (ND_s^- or ND_s^{*-}) for $I(J^P) = 1/2(1/2^-)$ in QDCSM. (a) stands for three-channel coupling with $\Sigma\bar{D}$, $\Sigma^*\bar{D}^*$, and ND_s^{*-}, (b) shows three-channel coupling with $\Sigma\bar{D}$, $\Sigma^*\bar{D}^*$, and ND_s^-.

- Only one resonance state $\Sigma\bar{D}$ appears in the scattering phase shifts of ND_s^- and ND_s^{*-}

Results of the Anticharmed-Strange Pentaquark

➤ Resonance state and decay width

$I = \frac{3}{2}$

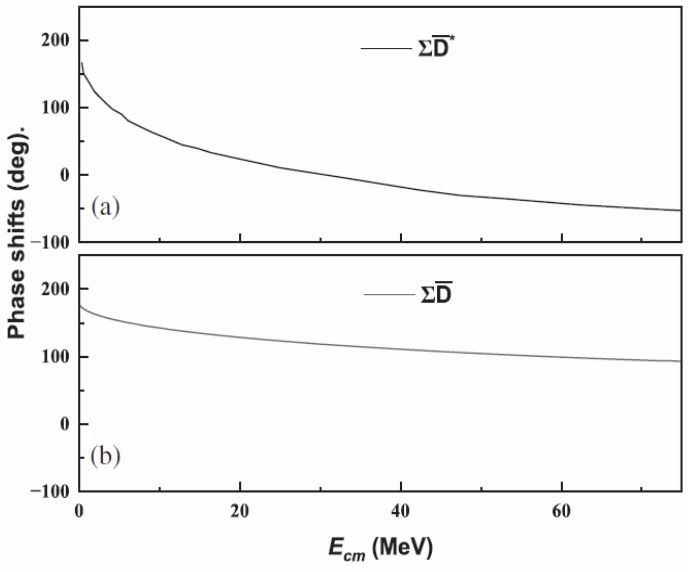

FIG. 7. The phase shifts of the open channels with two channels coupling with a closed channel (ΔD_s^{*-}) and one open channel ($\Sigma\bar{D}$, $\Sigma\bar{D}^*$) for $I(J^P) = 3/2(1/2^-)$ in QDCSM. (a) indicates two-channel coupling with ΔD_s^{*-} and $\Sigma\bar{D}$, (b) presents two-channel coupling with ΔD_s^{*-} and $\Sigma\bar{D}^*$.

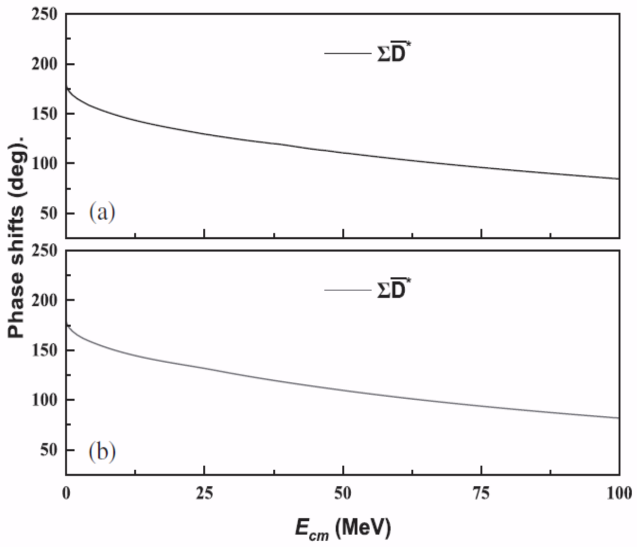

FIG. 8. The phase shifts of the open channels with two channels coupling with a closed channel (ΔD_s^-, ΔD_s^{*-}) and one open channel ($\Sigma\bar{D}^*$) for $I(J^P) = 3/2(3/2^-)$ in QDCSM. (a) Represents two channels coupling with ΔD_s^{*-} and $\Sigma\bar{D}^*$, (b) denotes two channels coupling with ΔD_s^- and $\Sigma\bar{D}^*$.

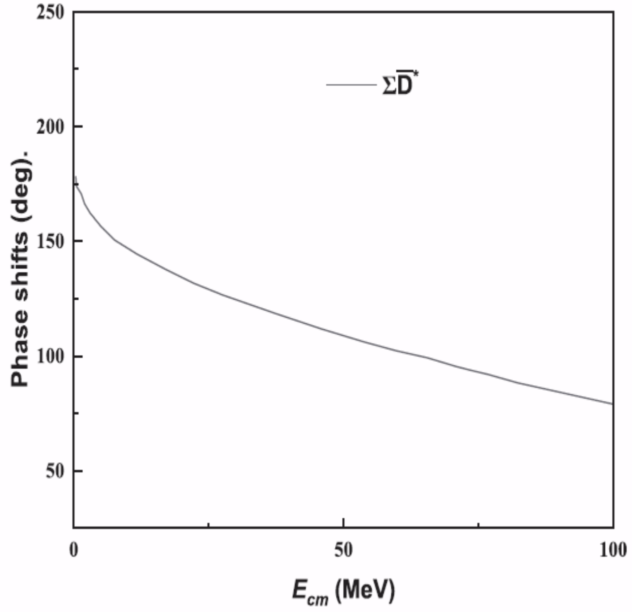

FIG. 9. The phase shifts of the open channels with three channels coupling with two closed channels (ΔD_s^-, ΔD_s^{*-}) and one open channel ($\Sigma\bar{D}^*$) for $I(J^P) = 3/2(3/2^-)$ in QDCSM.

- No resonance states can be observed in the corresponding scattering phase shifts

Results of the Anticharmed-Strange Pentaquark

➢ Resonance state and decay width

TABLE V. The masses and decay widths (in the unit of MeV) of resonance states with the difference scattering process. M_R^{th} stands for the sum of the corresponding theoretical threshold of the open channel and the incident energy, M_R represents the modified resonance mass. Γ_i is the partial decay width of the resonance state decaying to the ith open channel. Γ_{Total} is the total decay width of the resonance state.

	Three-channel coupling						Two-channel coupling								
	$I(J^P)=\frac{1}{2}(\frac{1}{2}^-)$						$I(J^P)=\frac{1}{2}(\frac{1}{2}^-)$						$I(J^P)=\frac{1}{2}(\frac{3}{2}^-)$		
	$\Sigma\bar{D}$			$\Sigma^*\bar{D}^*$			$\Sigma\bar{D}$			$\Sigma^*\bar{D}^*$			$\Sigma^*\bar{D}$		
Open channels	M_R^{th}	M_R	Γ_i	M_R^{th}	M_R	Γ_i	M_R^{th}	M_R	Γ_i	M_R^{th}	M_R	Γ_i	M_R^{th}	M_R	Γ_i
ND_s^-	3097	3053	5.5	…	…	…	3098	3054	5.6	…	…	…	…	…	…
ND_s^{*-}	3098	3054	7.5	…	…	…	3099	3055	7.8	…	…	…	…	…	…
$\Lambda\bar{D}$	…	…	…	…	…	…	…	…	…	3258	3390	1.1	…	…	…
$\Lambda\bar{D}^*$	…	…	…	…	…	…	…	…	…	…	…	…	3220	3250	1.3
$\Sigma\bar{D}^*$	…	…	…	…	…	…	…	…	…	3257	3389	9.5	3222	3252	3.1
Γ_{Total}			13.0						13.4			10.4			4.4

Three resonance states:

- $I(J^P)=\frac{1}{2}\left(\frac{1^-}{2}\right)$ $\Sigma\bar{D}$
- $I(J^P)=\frac{1}{2}\left(\frac{1^-}{2}\right)$ $\Sigma^*\bar{D}^*$
- $I(J^P)=\frac{1}{2}\left(\frac{3^-}{2}\right)$ $\Sigma^*\bar{D}$

Results of the Anticharmed-Strange Pentaquark

➢ Experimental potential

TABLE VI. The possible decay channels of Bound states and resonance states.

$I(J^P)$	Bound states	Possible decay channel
$\frac{1}{2}(\frac{3}{2}^-)$	ND_s^{*-}	ND_s^- (D-wave)
$\frac{3}{2}(\frac{3}{2}^-)$	$\Sigma\bar{D}^*$	$\Sigma\bar{D}$ (D-wave)
$I(J^P)$	Resonance states	Possible decay channel
$\frac{1}{2}(\frac{1}{2}^-)$	$\Sigma\bar{D}$	ND_s^-, ND_s^{*-}
	$\Sigma^*\bar{D}^*$	$\Lambda\bar{D}$, $\Sigma\bar{D}^*$
$\frac{1}{2}(\frac{3}{2}^-)$	$\Sigma^*\bar{D}$	$\Lambda\bar{D}^*$, $\Sigma\bar{D}^*$, $\Sigma\bar{D}$ (D-wave)

Summary

- Prediction of three bound states: our dynamical calculations predict the existence of three bound states：
  - $I(J^P) = \frac{1}{2}\left(\frac{1^-}{2}\right)$ with a predicted mass of 2886 MeV.
  - $I(J^P) = \frac{1}{2}\left(\frac{3^-}{2}\right)$ with a predicted mass of 3039 MeV.
  - $I(J^P) = \frac{3}{2}\left(\frac{3^-}{2}\right)$ with a predicted mass of 3153 MeV.
- Prediction of three resonance states: by analyzing scattering phase shifts, three resonance states are identified:
  - $\Sigma\bar{D}$ resonance $I(J^P) = \frac{1}{2}\left(\frac{1^-}{2}\right)$ with a mass of 3053-3055 MeV and a width of 13-13.4 MeV
  - $\Sigma^*\bar{D}^*$resonance $I(J^P) = \frac{1}{2}\left(\frac{1^-}{2}\right)$ with a mass of 3389-3390 MeV and a width of 10.4 MeV
  - $\Sigma^*\bar{D}$ resonance $I(J^P) = \frac{1}{2}\left(\frac{3^-}{2}\right)$ with a mass of 3250-3252 MeV and a width of 4.4 MeV

Thank you!